ADVANCED MATERIALS
www.advmat.de

Materials Views
www.MaterialsViews.com

Molecular Lock: A Versatile Key to Enhance Efficiency and Stability of Organic Solar Cells

Pei Cheng, Cenqi Yan, Tsz-Ki Lau, Jiangquan Mai, Xinhui Lu, and Xiaowei Zhan**

Due to the gradual depletion and environmental problem of traditional fossil energy sources, developing renewable clean energy technologies has become the focus of the 21st century. Especially, bulk heterojunction organic solar cells (OSCs) have attracted considerable attention in recent years because they present some advantages, such as low cost, light weight, flexibility, and large-area fabrication.[1–9] For both academic and industrial purposes, obtaining high power conversion efficiency (PCE) and good stability is the major goal for OSCs.

Numerous strategies have been employed to achieve high PCE: synthesizing new electron donor/acceptor materials;[10–17] incorporating a third component in active layer (ternary blend);[18–34] using thermal or solvent annealing, volatile or nonvolatile additives and layer-by-layer solution process to control the morphology of active layer;[35–40] employing interlayers or invert structures;[41,42] and fabricating tandem or parallel structure.[43,44]

Compared with achieving high PCE, there is much less study on device stability although it is also very important.[45,46] In recent years, researchers have started to pay more attention to this important issue and developed some strategies to improve device stability, such as purifying materials to reduce burn-in loss or remove organic impurities,[47,48] employing air stable electrode like gold, silver, or copper to replace calcium/aluminum mixed cathode,[49,50] using nonfullerene acceptors to replace fullerene acceptors which are easy to aggregate under light, thermal, or long-term conditions,[51,52] and employing modified or crosslinked fullerenes as a third component to suppress the excessive aggregation of [6,6]-phenyl-C61-butyric-acid-methyl-ester (PCBM).[53,54]

However, there are rare methods to improve efficiency and stability of OSCs simultaneously. For example, solvent additives such as 1,8-diiodooctane (DIO) and chloronaphthalene are used in OSCs to improve PCE, but they seriously reduce the device stability.[55–58] Nonfullerene acceptors are developed to replace fullerene acceptors since they can enhance device stability and lower cost,[59] but afford lower PCEs than fullerene counterpart.[60]

Most of the widely used, highly efficient, and classical donors contain fluorine (F) atoms, such as PTB7,[61] PTB7-th,[62] PffBT4T-2OD,[12] and p-DTS(FBTTh$_2$)$_2$.[63] For future industrial production, a simple, general, and effective approach that can simultaneously enhance the efficiency and stability of OSCs based on these F-containing donors is highly desired.

In this work, we develop a novel and simple strategy to enhance the efficiency and stability of OSCs simultaneously. 4,4′-Biphenol (BPO; **Figure 1**a), a common, cheap chemical, is employed as a "molecular lock" in blends of F-containing polymer and small molecule donors and fullerene acceptors to lock donor via hydrogen bond formed between the donor and BPO. This versatile molecular lock can enhance the efficiency of OSCs by promoting aggregation of donor and improve the device stability by freezing morphology of the blended films (Figure 1b).

To test the molecular lock BPO and to investigate the effect of hydrogen bond, six classical polymer or small molecule donors are chosen to blend with fullerene acceptor PC$_{71}$BM (Figure 1a); four donors (PTB7, PTB7-th, PffBT4T-2OD, and p-DTS(FBTTh$_2$)$_2$) have F atoms and the other two (PBDTTT-C-T and P3HT) do not have. **Figure 2** shows the *J*–*V* curves and external quantum efficiency (EQE) spectra of devices based on donor (PTB7, PTB7-th, PffBT4T-2OD, or p-DTS(FBTTh$_2$)$_2$):PC$_{71}$BM without (binary) and with BPO (ternary) fresh-made and degraded under the illumination of an AM 1.5G solar simulator, 100 mW cm^{-2}. The stability tests were carried out at 130 °C for 120 min under nitrogen atmosphere, and the curves of PCE versus heating time are shown in Figure 2. We also investigated the effect of heating temperature and time on stability of solar cells under nitrogen atmosphere (Figure S1, Supporting Information). The corresponding *J*–*V* and EQE of devices based on PBDTTT-C-T or P3HT:PC$_{71}$BM and PBDTTT-C-T or P3HT:BPO: PC$_{71}$BM are presented in Figure S2 (Supporting Information). The average and best device characteristics are summarized in **Table 1** (the average data are calculated from

P. Cheng
Beijing National Laboratory for Molecular Sciences
CAS Key Laboratory of Organic Solids
Institute of Chemistry
Chinese Academy of Sciences
Beijing 100190, P. R. China
P. Cheng
University of Chinese Academy of Sciences
Beijing 100049, P. R. China
C. Yan, Prof. X. Zhan
Department of Materials Science and Engineering
College of Engineering
Key Laboratory of Polymer Chemistry and Physics of Ministry of Education
Peking University
Beijing 100871, P. R. China
E-mail: xwzhan@pku.edu.cn
T.-K. Lau, J. Mai, Dr. X. Lu
Department of Physics
Chinese University of Hong Kong
New Territories
Hong Kong, P. R. China
E-mail: xhlu@phy.cuhk.edu.hk

DOI: 10.1002/adma.201600426

© 2016 WILEY-VCH Verlag GmbH & Co. KGaA, Weinheim

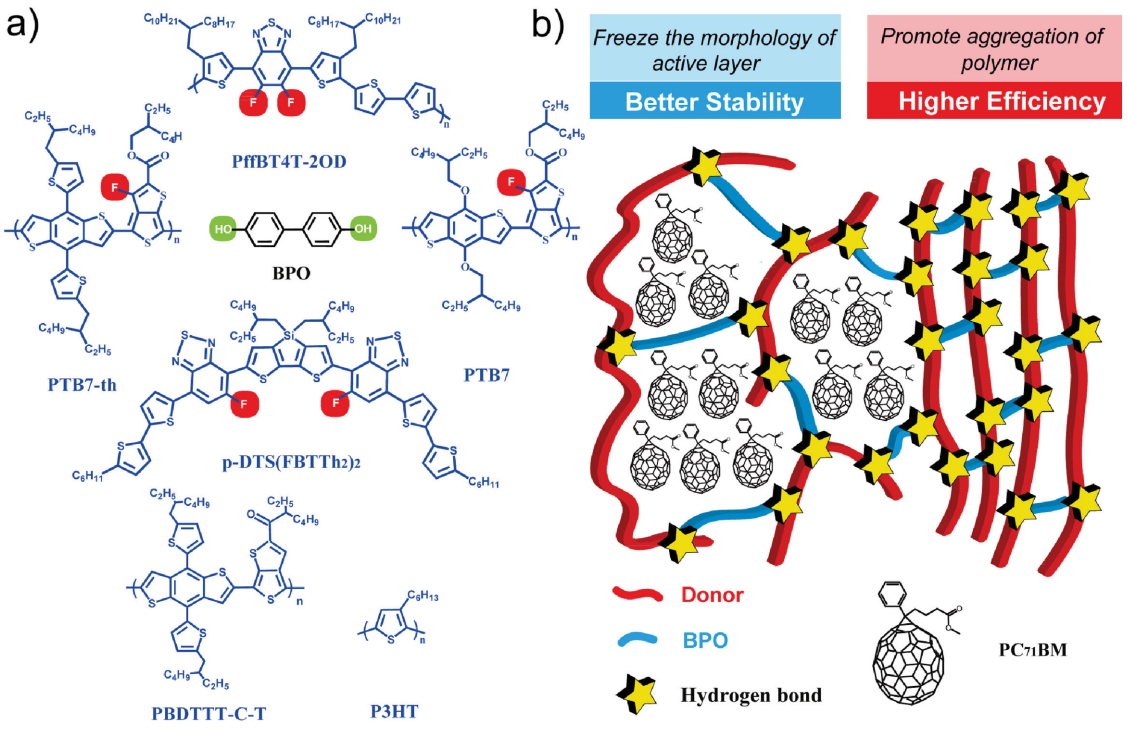

Figure 1. a) Molecular structures of PTB7, PTB7-th, PffBT4T-2OD, p-DTS(FBTTh$_2$)$_2$, PBDTTT-C-T, P3HT, and BPO. b) Schematic illustration of donor, PC$_{71}$BM, BPO, and hydrogen bond in active layer.

20 individual devices). For F-containing donor/fullerene solar cells (PTB7:PC$_{71}$BM, PTB7-th:PC$_{71}$BM, PffBT4T-2OD:PC$_{71}$BM, and p-DTS(FBTTh$_2$)$_2$:PC$_{71}$BM), the addition of BPO increases the short circuit current density (J_{SC}) and fill factor (FF), but slightly affects the open circuit voltage (V_{OC}). With increasing the BPO content (weight ratio of BPO in total weight of the donor, acceptor, and BPO) from 1.5% to 4.5%, the average J_{SC} and PCE increase first and then decrease (Table S1, Supporting Information). The F-containing donor/fullerene solar cells exhibit the best performance with addition of 3% BPO. After the addition of 3% BPO, the average PCE of PTB7:PC$_{71}$BM-based devices increases from 7.35% to 7.87%; the average PCE of PTB7-th:PC$_{71}$BM-based devices increases from 8.33% to 8.88%; the average PCE of PffBT4T-2OD:PC$_{71}$BM-based devices increases from 7.69% to 8.36%; and the average PCE of p-DTS(FBTTh$_2$)$_2$:PC$_{71}$BM-based devices increases from 6.44% to 7.02%. In contrast, the PCEs for donors without F atoms almost keep unchanged with the addition of 3% BPO (7.14% vs 7.14% for PBDTTT-C-T:PC$_{71}$BM-based devices and 3.84% vs 3.83% for P3HT:PC$_{71}$BM-based devices).

After heating at 130 °C for 120 min, the PCE of PTB7:PC$_{71}$BM-based devices without BPO decays from 7.35% to 2.96%; the PCE of PTB7-th:PC$_{71}$BM-based devices without BPO decays from 8.33% to 3.95%; the PCE of PffBT4T-2OD:PC$_{71}$BM-based devices without BPO decays from 7.69% to 4.08%; and the PCE of p-DTS(FBTTh$_2$)$_2$:PC$_{71}$BM-based devices without BPO decays from 6.44% to 2.25%, preserving only 40%, 47%, 53%, and 35% of its original value, respectively. The addition of 3% BPO improves the stability of F-containing donor/fullerene solar cells (Figure 2c,f,i,l). After heating at 130 °C for 120 min, the PCE of PTB7:BPO:PC$_{71}$BM-based devices decays from 7.87% to 6.26%; the PCE of PTB7-th:BPO:PC$_{71}$BM-based devices decays from 8.88% to 6.86%; the PCE of PffBT4T-2OD:BPO:PC$_{71}$BM-based devices decays from 8.36% to 6.80%; and the PCE of p-DTS(FBTTh$_2$)$_2$:BPO:PC$_{71}$BM-based devices decays from 7.02% to 5.28%, preserving 80%, 77%, 81%, and 75% of its original value, respectively. Figure S3 (Supporting Information) shows stability curves of PTB7:PC$_{71}$BM-based devices with different contents of BPO under heating at 130 °C for 120 min (Supporting Information). With the addition of different contents of BPO (1.5%, 3%, and 4.5%), the devices show similar stability properties (preserving ≈80% of its original PCE).

For donor/fullerene solar cells without F atoms (PBDTTT-C-T:PC$_{71}$BM and P3HT:PC$_{71}$BM), the addition of 3% BPO does not improve the device stability. The PCE of the devices based on PBDTTT-C-T:PC$_{71}$BM and P3HT:PC$_{71}$BM blends without BPO preserves 46% and 52% of its original value, while that with BPO preserves 49% and 53% of its original value after heating at 130 °C for 120 min, respectively.

As shown in Figure 2b,e,h,k, the trend of EQE is similar to J_{SC}. The EQE in the range of 450–750 nm is mainly contributed by PTB7, PTB7-th, PffBT4T-2OD, or p-DTS(FBTTh$_2$)$_2$, while that below 450 nm is mainly contributed by PC$_{71}$BM. The EQE related to PTB7, PTB7-th, PffBT4T-2OD, or p-DTS(FBTTh$_2$)$_2$ is enhanced by adding 3% BPO. Our degradation process dramatically decreases the EQE of donor (PTB7, PTB7-th, PffBT4T-2OD, or p-DTS(FBTTh$_2$)$_2$):PC$_{71}$BM-based devices, while slightly decreases the EQE of donor (PTB7, PTB7-th, PffBT4T-2OD, or p-DTS(FBTTh$_2$)$_2$):BPO:PC$_{71}$BM-based devices. The calculated J_{SC} values obtained from the integration of the EQE spectra with the AM 1.5G reference spectrum are closed to the measured values (the average mismatch is 2.2%; Table 1).

© 2016 WILEY-VCH Verlag GmbH & Co. KGaA, Weinheim

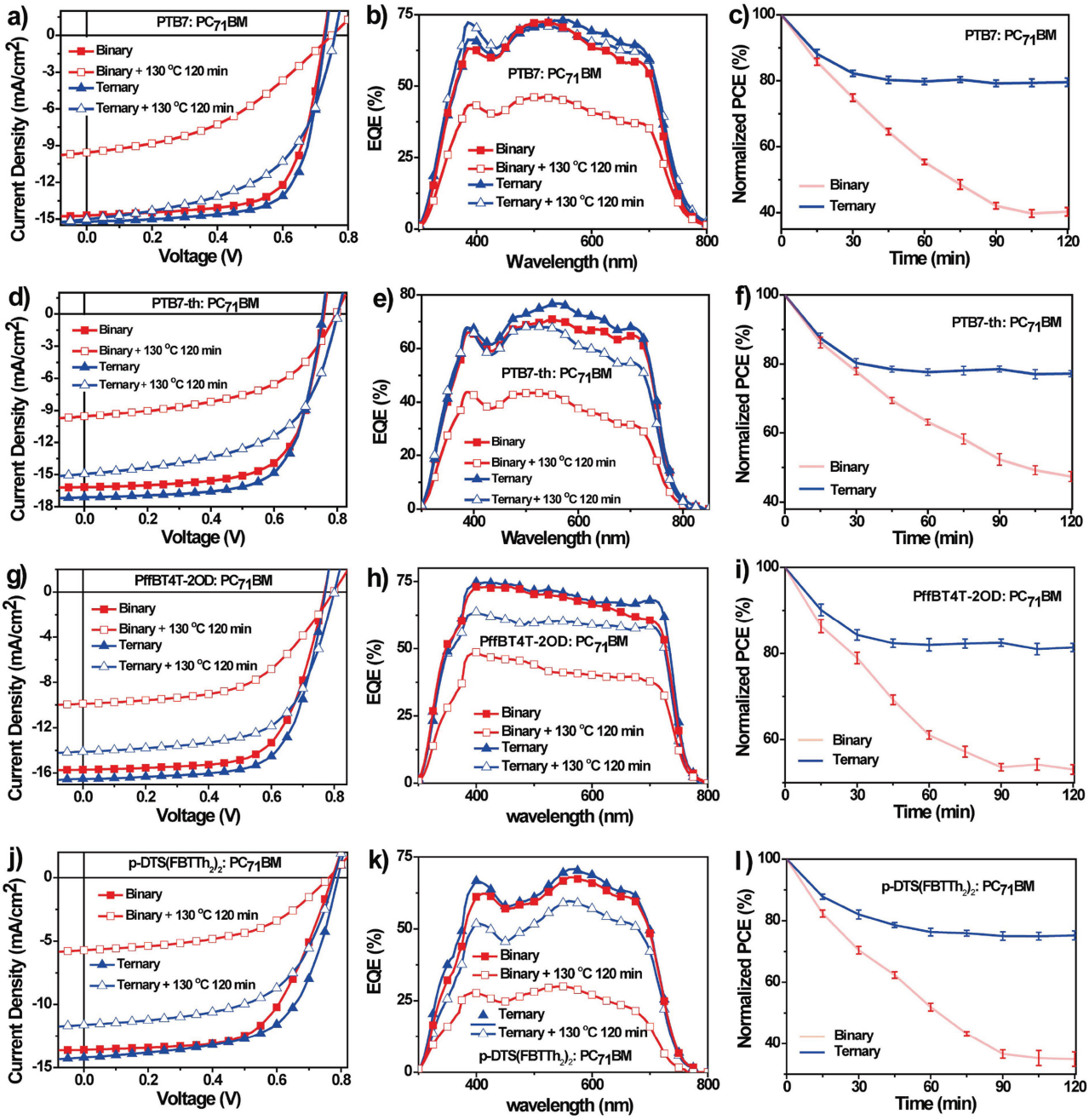

Figure 2. a,d,g,j) *J–V* curves and b,e,h,k) EQE spectra of devices with the structure ITO/PEDOT:PSS/(PTB7, PTB7-th, PffBT4T-2OD, or p-DTS(FBTTh$_2$)$_2$):PC$_{71}$BM/Ca/Al without and with BPO before and after heating at 130 °C for 120 min under the illumination of an AM 1.5G solar simulator, 100 mW cm^{-2}. c,f,i,l) Stability curves of (PTB7, PTB7-th, PffBT4T-2OD, or p-DTS(FBTTh$_2$)$_2$):PC$_{71}$BM devices without and with BPO under continuous heating at 130 °C for 120 min.

Fourier transform infrared (FTIR) spectroscopy measurements are carried out to probe hydrogen bond between F-containing donor and BPO in blended films. **Figure 3** shows FTIR spectra of PBDTTT-C-T:PC$_{71}$BM, PBDTTT-C-T:BPO:PC$_{71}$BM, PTB7:PC$_{71}$BM, and PTB7:BPO:PC$_{71}$BM blended films before and after heating at 130 °C for 120 min. Relative to PBDTTT-C-T:PC$_{71}$BM blend, a new peak at 3392 cm^{-1} is observed for PBDTTT-C-T:BPO:PC$_{71}$BM blend, which is attributed to O—H...O hydrogen bond formed between BPO molecules.[64] After heating at 130 °C for 120 min, this peak disappears, suggesting the hydrogen bond is broken. In PTB7:PC$_{71}$BM blend, the addition of BPO leads to the occurrence of a new peak at 3268 cm^{-1}, due to the formation of O—H...F hydrogen bond between PTB7 and BPO. Interestingly, after heating at 130 °C for 120 min, this peak is still observed but becomes weaker since O—H...F hydrogen bond is stronger than O—H...O hydrogen bond. Because one BPO molecule has two hydroxyl groups and one polymer chain has many F atoms, the O—H...F hydrogen bond

© 2016 WILEY-VCH Verlag GmbH & Co. KGaA, Weinheim

Table 1. Average and best device data based on donor: $PC_{71}BM$ blended films without and with BPO before and after heating at 130 °C for 120 min.

Active layer	BPO [%]	Heating time [min]	V_{OC} [V]	J_{SC} [mA cm^{-2}]	calc J_{SC} [mA cm^{-2}]	FF [%]	PCE [%]	
							Average	Best
PTB7:$PC_{71}BM$	0	0	0.728	14.7	14.5	68.7	7.35	7.42
PTB7:$PC_{71}BM$	0	120	0.750	9.56	9.35	41.3	2.96	3.05
PTB7:$PC_{71}BM$	3	0	0.732	15.2	15.0	70.7	7.87	8.03
PTB7:$PC_{71}BM$	3	120	0.760	15.0	14.7	54.9	6.26	6.38
PTB7-th:$PC_{71}BM$	0	0	0.758	16.2	16.0	67.8	8.33	8.51
PTB7-th:$PC_{71}BM$	0	120	0.797	9.58	9.25	51.7	3.95	4.11
PTB7-th:$PC_{71}BM$	3	0	0.754	17.1	16.9	68.9	8.88	9.06
PTB7-th:$PC_{71}BM$	3	120	0.804	15.0	14.7	56.9	6.86	7.12
PffBT4T-2OD:$PC_{71}BM$	0	0	0.745	15.7	15.5	65.6	7.69	8.01
PffBT4T-2OD: $PC_{71}BM$	0	120	0.773	9.87	9.60	53.5	4.08	4.33
PffBT4T-2OD: $PC_{71}BM$	3	0	0.748	16.5	16.2	67.7	8.36	8.54
PffBT4T-2OD: $PC_{71}BM$	3	120	0.775	14.1	13.7	62.2	6.80	7.08
p-DTS$(FBTTh_2)_2$: $PC_{71}BM$	0	0	0.773	13.6	13.3	61.3	6.44	6.71
p-DTS$(FBTTh_2)_2$: $PC_{71}BM$	0	120	0.762	5.71	5.58	51.7	2.25	2.48
p-DTS$(FBTTh_2)_2$: $PC_{71}BM$	3	0	0.791	14.2	13.8	62.5	7.02	7.13
p-DTS$(FBTTh_2)_2$: $PC_{71}BM$	3	120	0.780	11.6	11.4	58.4	5.28	5.63
PBDTTT-C-T: $PC_{71}BM$	0	0	0.760	14.9	14.6	62.9	7.14	7.26
PBDTTT-C-T: $PC_{71}BM$	0	120	0.778	8.32	8.09	50.7	3.28	3.40
PBDTTT-C-T: $PC_{71}BM$	3	0	0.762	14.6	14.4	64.2	7.14	7.22
PBDTTT-C-T: $PC_{71}BM$	3	120	0.776	8.80	8.61	51.1	3.49	3.57
P3HT: $PC_{71}BM$	0	0	0.626	9.20	9.03	66.5	3.83	4.05
P3HT: $PC_{71}BM$	0	120	0.547	6.83	6.55	53.0	1.98	2.14
P3HT: $PC_{71}BM$	3	0	0.627	9.11	8.89	67.3	3.84	4.03
P3HT: $PC_{71}BM$	3	120	0.527	7.54	7.30	51.1	2.03	2.22

facilitates the formation of dense network among polymer chains as illustrated in Figure 1.

In order to understand the effect of BPO on film morphology, grazing-incidence wide-angle and small-angle X-ray scattering (GIWAXS and GISAXS) measurements are carried out. GIWAXS provides molecular-level structural information such as lattice constant and orientation of polymer packing,[65,66] while GISAXS provides larger length-scale phase separation information up to hundreds nanometers.[62,67] **Figure 4**a shows 2D GIWAXS patterns of PTB7:$PC_{71}BM$ and PTB7:BPO:$PC_{71}BM$ blended films before and after heating at 130 °C for 120 min. In contrast to the films without BPO, both the films with BPO fresh-made and heated show an obvious π–π stacking peak (q ≈1.7 Å^{-1}) along the q_z-axis, indicating an enhanced π–π ordering in "face-on" orientated polymer domains induced by the addition of BPO. Strong "face-on" oriented π–π stacking was reported for pure PTB7 film previously.[34] However, after blended with $PC_{71}BM$, this π–π ordering is greatly reduced as indicated by the disappearance of π–π stacking peak (Figure 4a). Thus, the observation of "face-on" π–π stacking in the ternary films must result from the addition of BPO. It might be reasonably attributed to the hydrogen bonds formed between polymer and BPO that provide more driving force for π–π stacking (not obvious in PBDTTT-C-T:BPO:$PC_{71}BM$ films; Figure S4, Supporting Information). Note that the strong O—H...F bond formed in PTB7:BPO:$PC_{71}BM$ system could survive after heating and contribute to the remarkably stable device performance.

Figure 4b presents the corresponding 2D GISAXS patterns. The in-plane scattering intensity profiles are shown in Figure 4c. By fitting them with the model adopted by Liao et al.[62] we could roughly estimate the average domain size of $PC_{71}BM$ clusters (R_g_$PC_{71}BM$). For PTB7:BPO:$PC_{71}BM$ system, it remains unchanged (≈12 nm) before and after heating. However, it increases from ≈7 to ≈19 nm for PBDTTT-C-T:BPO:$PC_{71}BM$ system. The hydrogen bond can induce stable polymer networks which can suppress the diffusing of fullerenes during continuous heating, resulting in the unchanged domain size of $PC_{71}BM$ clusters. Since the device performance could be very sensitive to the domain size of $PC_{71}BM$,[68] this also supports the observed stable device performance of PTB7:BPO:$PC_{71}BM$ system under heating.

Figure 5a shows the ultraviolet–visible (UV–vis) absorption spectra of PTB7:$PC_{71}BM$ and PTB7:BPO:$PC_{71}BM$ blended films with similar thickness (≈100 nm) before and after heating at 130 °C for 120 min. After the addition of BPO in PTB7:$PC_{71}BM$ blended

© 2016 WILEY-VCH Verlag GmbH & Co. KGaA, Weinheim

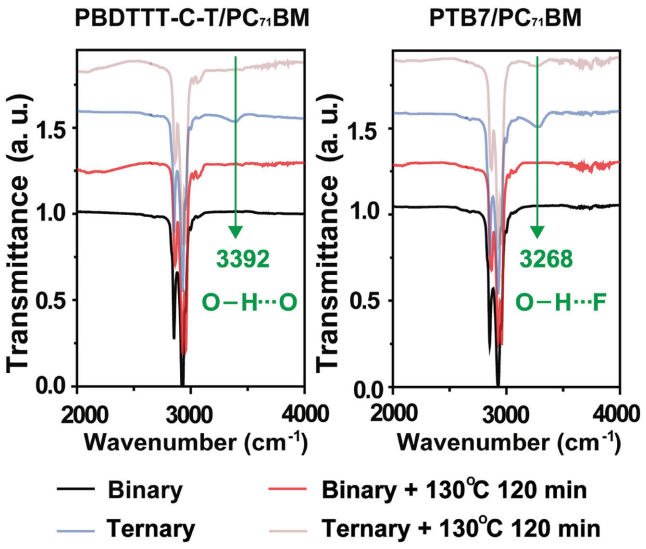

Figure 3. FTIR spectra of PBDTTT-C-T:$PC_{71}BM$, PBDTTT-C-T:BPO:$PC_{71}BM$ (left) and PTB7:$PC_{71}BM$, PTB7:BPO:$PC_{71}BM$ (right) blended films before and after heating at 130 °C for 120 min.

film, the absorption between 500 and 700 nm is enhanced. This enhancement is attributed to the significantly enhanced absorption of polymer donor (Figure 5b). In contrast, the absorption of PBDTTT-C-T film slightly changes after the addition of BPO. Seen from GIWAXS, the hydrogen bond between PTB7 and BPO enhances the π–π stacking of polymer donor, which is the reason for the enhanced absorption of PTB7:BPO:$PC_{71}BM$ relative to PTB7:$PC_{71}BM$. After heating at 130 °C for 120 min, the absorption of PTB7:BPO:$PC_{71}BM$ blended film decreases slightly relative to that of PTB7:$PC_{71}BM$ blended film, indicating that BPO freezes the polymer aggregate state.

The hole mobility and electron mobility of PTB7:$PC_{71}BM$ and PTB7:BPO:$PC_{71}BM$ blended films before and after heating at 130 °C for 120 min are measured by space charge limited current[69] method (Figure 5c,d and Table S2, Supporting Information). Hole-only and electron-only diodes are fabricated using the architectures: ITO/PEDOT:PSS/active layer/Au for holes and Al/active layer/Al for electrons. The hole mobility increases with the addition of BPO (9.05×10^{-3} vs 3.48×10^{-3} cm^2 V^{-1} s^{-1}), while the electron mobility is slightly changed. The hydrogen bond between PTB7 and BPO leads to strong interchain interactions of polymer chains and dense polymer networks, which is beneficial to the improvement of hole mobility. After heating at 130 °C for 120 min, the hole mobility of PTB7:$PC_{71}BM$ blended film decreases by one order of magnitude (3.42×10^{-4} vs 3.48×10^{-3} cm^2 V^{-1} s^{-1}), while the hole mobility of PTB7:BPO:$PC_{71}BM$ blended film decreases to a less extent (5.25×10^{-3} vs 9.05×10^{-3} cm^2 V^{-1} s^{-1}), because the hydrogen bond between PTB7 and BPO facilitates the formation of polymer network.

In order to investigate the vertical phase separation of blended films, we use X-ray photoelectron spectroscopy (XPS) to measure the ratio of atoms and estimate donor/acceptor ratios at top surface. To confirm whether the ion etching by XPS test is uniform or not, we carried out atomic force microscopy measurement (Figure S5, Supporting Information). After

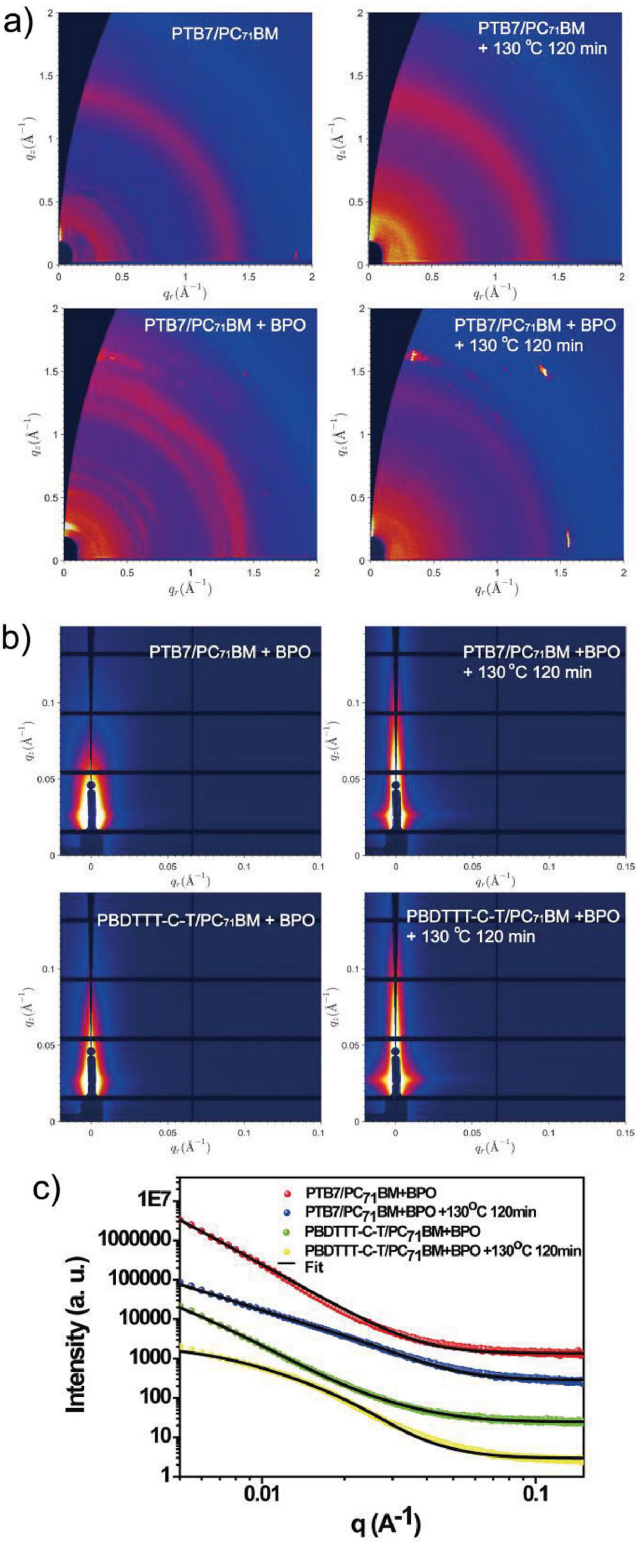

Figure 4. a) 2D GIWAXS patterns of PTB7:$PC_{71}BM$, PTB7:BPO:$PC_{71}BM$ blended films before and after heating at 130 °C for 120 min. b) 2D GISAXS patterns of PTB7:BPO:$PC_{71}BM$ and PBDTTT-C-T:BPO:$PC_{71}BM$ before and after heating at 130 °C for 120 min. c) The corresponding GISAXS profiles and best fittings along the in-plane.

© 2016 WILEY-VCH Verlag GmbH & Co. KGaA, Weinheim

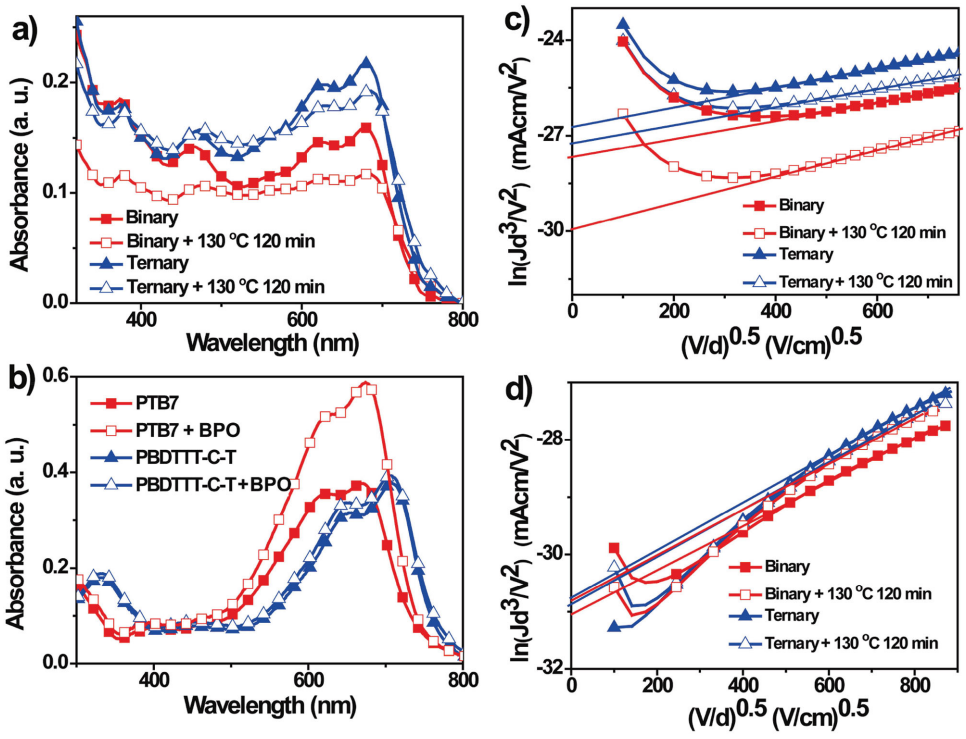

Figure 5. UV–vis absorption spectra of a) PTB7:$PC_{71}BM$ and PTB7:BPO:$PC_{71}BM$ blended films before and after heating at 130 °C for 120 min and b) PTB7 and PBDTTT-C-T films without or with BPO. *J–V* characteristics under dark for c) hole-only and d) electron-only devices based on PTB7:$PC_{71}BM$ and PTB7:BPO:$PC_{71}BM$ blend films before and after heating at 130 °C for 120 min.

ion etching by XPS test, the film is still uniform and smooth. The root-mean-square roughness is less than 1 nm, which is far below the distance of ion etching by XPS test (≈10 nm). XPS survey scans of PTB7:$PC_{71}BM$ and PTB7:BPO:$PC_{71}BM$ blended films before and after heating at 130 °C for 120 min are shown in Figure S6 (Supporting Information). Since PTB7 contains sulfur and PTB7, BPO, and $PC_{71}BM$ contain oxygen, we attribute the sulfur 2p (S 2p) spectral line (≈160 eV) to PTB7 and oxygen 1s (O 1s) spectral line (≈530 eV) to PTB7, BPO, and $PC_{71}BM$. One repeated unit of PTB7 contains four S atoms and four O atoms, while one BPO or $PC_{71}BM$ molecule contains two O atoms. Top surface compositions of PTB7:$PC_{71}BM$ and PTB7:BPO:$PC_{71}BM$ blended films can be calculated from the O/S ratio (Table S3, Supporting Information). The top surface molar content of PTB7 decreases from 41.3% to 30.1% with the addition of BPO, as dense polymer network formed via the hydrogen bond suppresses the migration of polymers to the top surface. As a result, smaller polymer donor content at top surface is beneficial to electron collection at cathode. After heating at 130 °C for 120 min, the top surface molar content of PTB7 in PTB7:$PC_{71}BM$ blended film decreases from 41.3% to 30.5% due to the excessive aggregation of $PC_{71}BM$ on the top surface caused by continuous heating. For PTB7:BPO:$PC_{71}BM$ blended film, heating leads to a little change in PTB7 molar content (29.6% vs 30.1%) because the hydrogen bond between PTB7 and BPO freezes the morphology of active layer.

In summary, the molecular lock BPO is employed as the dual functional third component in F-containing donor/fullerene blends. Through hydrogen bond between F-containing donor and BPO, the donors are interconnected, the dense donor network is formed, and the film morphology is frozen. The absorption and hole mobility of active layer are enhanced due to enhanced π–π stacking and aggregation of donor. Moreover, the vertical phase separation of active layer is optimized since dense donor network suppresses the migration of donors to the top surface. Enhanced absorption, higher hole mobility, and optimized vertical phase separation lead to higher PCE of OSCs. Furthermore, the stability of OSCs is enhanced since the hydrogen bond freezes the donor aggregate state and suppresses the excessive aggregation of $PC_{71}BM$. Our results demonstrate that molecular lock is a versatile key to enhance efficiency and stability of organic solar cells simultaneously.

Experimental Section

Unless stated otherwise, solvents and chemicals were obtained commercially and used without further purification. PTB7,[61] PTB7-th,[62] and p-DTS(FBTTh$_2$)$_2$[63] were purchased from One-Materials Inc.; PBDTTT-C-T[70] and PffBT4T-2OD[12] were purchased from Solarmer Materials Inc.; P3HT was purchased from Rieke Metals Inc.; and $PC_{71}BM$ (purity > 99.0%) was purchased from American Dye Inc. DIO, chlorobenzene (CB), and *o*-dichlorobenzene (DCB) were obtained from J&K Chemical Inc. Organic solar cells were fabricated with the structure: ITO/PEDOT:PSS/active layer/Ca/Al. The ITO glass (sheet resistance = 10 Ω□$^{-1}$) was precleaned in an ultrasonic bath of acetone and isopropanol, and treated in ultraviolet-ozone chamber (Jelight Company, USA) for 20 min. A thin layer (35 nm) of PEDOT:PSS (Baytron PVP AI 4083, Germany) was spin-coated onto the ITO glass and baked at 150 °C for 20 min. A mixture of

© 2016 WILEY-VCH Verlag GmbH & Co. KGaA, Weinheim

PTB7 or PTB7-th or PBDTTT-C-T:$PC_{71}BM$ was dissolved in DCB solvent (1:1.5, 25 mg mL^{-1} in total) with stirring overnight. Then, this polymer/fullerene solution with 3% DIO with or without 1.5% or 3% or 4.5% BPO was spin-coated on the PEDOT:PSS layer to form a photosensitive layer. Similarly, a mixture of PffBT4T-2OD:$PC_{71}BM$ was dissolved in DCB/CB 1:1 mixed solvent (1:1.2, 15.4 mg mL^{-1} in total) with stirring and heating overnight. Then, this polymer/fullerene solution with 3% DIO with or without 3% BPO was spin-coated on the PEDOT:PSS layer to form a photosensitive layer. A mixture of p-DTS$(FBTTh_2)_2$:$PC_{71}BM$ was dissolved in CB solvent (1.5:1, 35 mg mL^{-1} in total) with stirring and heating overnight. Then, this small molecule/fullerene solution with 0.4% DIO with or without 3% BPO was spin-coated on the PEDOT:PSS layer to form a photosensitive layer. A mixture of P3HT:$PC_{71}BM$ was dissolved in DCB solvent (1:1, 40 mg mL^{-1} in total) with stirring overnight. Then, this solution with or without 3% BPO was spin-coated on the PEDOT:PSS layer to form a photosensitive layer. The thickness of active layer was ranging from 90 to 300 nm, as measured by Ambios Technology XP-2 profilometer. A Ca (≈20 nm) and Al layer (≈80 nm) was then evaporated onto the surface of the photosensitive layer under vacuum (≈10^{-5} Pa) to form the negative electrode. The active area of the device was 4 mm^2. The *J–V* curve was measured using a computer-controlled B2912A Precision Source/Measure Unit (Agilent Technologies). An XES-70S1 (SAN-EI Electric Co., Ltd.) solar simulator (AAA grade, 70 × 70 mm^2 photobeam size) coupled with AM 1.5G solar spectrum filters was used as the light source, and the optical power at the sample was 100 mW cm^{-2}. A 2 × 2 cm^2 monocrystalline silicon reference cell (SRC-1000-TC-QZ) was purchased from VLSI Standards Inc. The EQE spectrum was measured using a Solar Cell Spectral Response Measurement System QE-R3011 (Enlitech Co., Ltd.). The light intensity at each wavelength was calibrated using a standard single crystal Si photovoltaic cell.

Stability test of solar cells was carried out at room temperature or under continuous heating at 110, 130, or 150 °C for 2, 24, or 336 h, and the *J–V* was measured using a B2912A source meter under AM 1.5G illumination. These tests were carried out in glove box. FTIR studies were performed using a Bruker Tensor 27 FTIR spectrometer. The grazing incidence X-ray scattering measurements (GIWAXS and GISAXS) were carried out at BL23A1 of National Synchrotron Radiation Research Center, Hsinchu. The energy of the X-ray source was set to 10 keV (wavelength of 1.24 Å) and the incident angle was 0.15°. Thin-film (on quartz substrate) UV–vis absorption spectra were recorded on a JASCO V-570 spectrophotometer. Hole-only or electron-only diodes were fabricated using the architectures: ITO/PEDOT:PSS/active layer/Au for holes and Al/active layer/Al for electrons. Mobilities were extracted by fitting the current density–voltage curves using the Mott–Gurney relationship (space charge limited current). XPS was performed on the Thermo Scientific ESCALab 250Xi using 200 W monochromated Al K_α radiation. The 500 µm X-ray spot was used for XPS analysis. The base pressure in the analysis chamber was about 3×10^{-10} mbar. Typically, the hydrocarbon C1s line at 284.8 eV from adventitious carbon was used for energy reference.

Supporting Information

Supporting Information is available from the Wiley Online Library or from the author.

Acknowledgements

X.Z. thanks the NSFC (Grant Nos. 51261130582 and 21025418) for financial support. X.L. acknowledges the financial support from Research Grant Council of Hong Kong (General Research Fund No. 2130394, Theme-based Research Scheme No. T23-407/13-N), and CUHK Focused Innovation Scheme B (No. 1902034).

Received: January 24, 2016
Revised: March 18, 2016
Published online: May 9, 2016

[1] C. J. Brabec, M. Heeney, I. McCulloch, J. Nelson, *Chem. Soc. Rev.* **2011**, *40*, 1185.
[2] L. Lu, T. Zheng, Q. Wu, A. M. Schneider, D. Zhao, L. Yu, *Chem. Rev.* **2015**, *115*, 12666.
[3] X. Guo, A. Facchetti, T. J. Marks, *Chem. Rev.* **2014**, *114*, 8943.
[4] P. Cheng, X. Zhan, *Chem. Soc. Rev.* **2016**, DOI: 10.1039/C5CS00593K.
[5] Y. Lin, Y. Li, X. Zhan, *Chem. Soc. Rev.* **2012**, *41*, 4245.
[6] M. Hösel, D. Angmo, R. R. Søndergaard, G. A. dos Reis Benatto, J. E. Carlé, M. Jørgensen, F. C. Krebs, *Adv. Sci.* **2014**, *1*, 1400002.
[7] Y.-J. Cheng, S.-H. Yang, C.-S. Hsu, *Chem. Rev.* **2009**, *109*, 5868.
[8] L. Dou, Y. Liu, Z. Hong, G. Li, Y. Yang, *Chem. Rev.* **2015**, *115*, 12633.
[9] Y. Huang, E. J. Kramer, A. J. Heeger, G. C. Bazan, *Chem. Rev.* **2014**, *114*, 7006.
[10] Y. F. Li, *Acc. Chem. Res.* **2012**, *45*, 723.
[11] Y. Lin, X. Zhan, *Acc. Chem. Res.* **2016**, *49*, 175.
[12] Y. Liu, J. Zhao, Z. Li, C. Mu, W. Ma, H. Hu, K. Jiang, H. Lin, H. Ade, H. Yan, *Nat. Commun.* **2014**, *5*, 5293.
[13] H.-Y. Chen, J. Hou, S. Zhang, Y. Liang, G. Yang, Y. Yang, L. Yu, Y. Wu, G. Li, *Nat. Photonics* **2009**, *3*, 649.
[14] S. C. Price, A. C. Stuart, L. Yang, H. Zhou, W. You, *J. Am. Chem. Soc.* **2011**, *133*, 4625.
[15] H. Zhou, L. Yang, A. C. Stuart, S. C. Price, S. Liu, W. You, *Angew. Chem. Int. Ed.* **2011**, *50*, 2995.
[16] Y. J. He, H. Y. Chen, J. H. Hou, Y. F. Li, *J. Am. Chem. Soc.* **2010**, *132*, 1377.
[17] Y. Lin, Q. He, F. Zhao, L. Huo, J. Mai, X. Lu, C. Su, T. Li, J. Wang, J. Zhu, Y. Sun, C. Wang, X. Zhan, *J. Am. Chem. Soc.* **2016**, *138*, 2973.
[18] P. P. Khlyabich, B. Burkhart, B. C. Thompson, *J. Am. Chem. Soc.* **2011**, *133*, 14534.
[19] P. P. Khlyabich, B. Burkhart, B. C. Thompson, *J. Am. Chem. Soc.* **2012**, *134*, 9074.
[20] R. A. Street, D. Davies, P. P. Khlyabich, B. Burkhart, B. C. Thompson, *J. Am. Chem. Soc.* **2013**, *135*, 986.
[21] T. Ameri, P. Khoram, J. Min, C. J. Brabec, *Adv. Mater.* **2013**, *25*, 4245.
[22] T. Ameri, T. Heumuller, J. Min, N. Li, G. Matt, U. Scherf, C. J. Brabec, *Energy Environ. Sci.* **2013**, *6*, 1796.
[23] M. Koppe, H. J. Egelhaaf, G. Dennler, M. C. Scharber, C. J. Brabec, P. Schilinsky, C. N. Hoth, *Adv. Funct. Mater.* **2010**, *20*, 338.
[24] L. Lu, T. Xu, W. Chen, E. S. Landry, L. Yu, *Nat. Photonics* **2014**, *8*, 716.
[25] L. Lu, M. A. Kelly, W. You, L. Yu, *Nat. Photonics* **2015**, *9*, 491.
[26] L. Lu, W. Chen, T. Xu, L. Yu, *Nat. Commun.* **2015**, *6*, 7327.
[27] L. Yang, H. Zhou, S. C. Price, W. You, *J. Am. Chem. Soc.* **2012**, *134*, 5432.
[28] Y. Yang, W. Chen, L. Dou, W.-H. Chang, H.-S. Duan, B. Bob, G. Li, Y. Yang, *Nat. Photonics* **2015**, *9*, 190.
[29] Y. Zhang, D. Deng, K. Lu, J. Zhang, B. Xia, Y. Zhao, J. Fang, Z. Wei, *Adv. Mater.* **2015**, *27*, 1071.
[30] J. Zhang, Y. Zhang, J. Fang, K. Lu, Z. Wang, W. Ma, Z. Wei, *J. Am. Chem. Soc.* **2015**, *137*, 8176.
[31] B. M. Savoie, S. Dunaisky, T. J. Marks, M. A. Ratner, *Adv. Energy Mater.* **2015**, *5*, 1400891.
[32] P. Cheng, X. Zhan, *Mater. Horiz.* **2015**, *2*, 462.
[33] P. Cheng, Y. Li, X. Zhan, *Energy Environ. Sci.* **2014**, *7*, 2005.
[34] P. Cheng, C. Yan, Y. Li, W. Ma, X. Zhan, *Energy Environ. Sci.* **2015**, *8*, 2357.
[35] P. Cheng, L. Ye, X. Zhao, J. Hou, Y. Li, X. Zhan, *Energy Environ. Sci.* **2014**, *7*, 1351.

© 2016 WILEY-VCH Verlag GmbH & Co. KGaA, Weinheim

[36] P. Cheng, J. Hou, Y. Li, X. Zhan, *Adv. Energy Mater.* **2014**, *4*, 1301349.
[37] G. Li, V. Shrotriya, J. S. Huang, Y. Yao, T. Moriarty, K. Emery, Y. Yang, *Nat. Mater.* **2005**, *4*, 864.
[38] X. Lu, H. Hlaing, D. S. Germack, J. Peet, W. H. Jo, D. Andrienko, K. Kremer, B. M. Ocko, *Nat. Commun.* **2012**, *3*, 795.
[39] Y. Sun, G. C. Welch, W. L. Leong, C. J. Takacs, G. C. Bazan, A. J. Heeger, *Nat. Mater.* **2012**, *11*, 44.
[40] Z. Xiao, Y. Yuan, B. Yang, J. VanDerslice, J. Chen, O. Dyck, G. Duscher, J. Huang, *Adv. Mater.* **2014**, *26*, 3068.
[41] Z. He, C. Zhong, S. Su, M. Xu, H. Wu, Y. Cao, *Nat. Photonics* **2012**, *6*, 591.
[42] Z. A. Page, Y. Liu, V. V. Duzhko, T. P. Russell, T. Emrick, *Science* **2014**, *346*, 441.
[43] A. R. b. M. Yusoff, D. Kim, H. P. Kim, F. K. Shneider, W. J. da Silva, J. Jang, *Energy Environ. Sci.* **2015**, *8*, 303.
[44] L. Zuo, C.-C. Chueh, Y.-X. Xu, K.-S. Chen, Y. Zang, C.-Z. Li, H. Chen, A. K. Y. Jen, *Adv. Mater.* **2014**, *26*, 6778.
[45] M. Jorgensen, K. Norrman, S. A. Gevorgyan, T. Tromholt, B. Andreasen, F. C. Krebs, *Adv. Mater.* **2012**, *24*, 580.
[46] E. Voroshazi, I. Cardinaletti, T. Conard, B. P. Rand, *Adv. Energy Mater.* **2014**, *4*, 1400848.
[47] J. Kong, S. Song, M. Yoo, G. Y. Lee, O. Kwon, J. K. Park, H. Back, G. Kim, S. H. Lee, H. Suh, K. Lee, *Nat. Commun.* **2014**, *5*, 5688.
[48] W. R. Mateker, J. D. Douglas, C. Cabanetos, I. T. Sachs-Quintana, J. A. Bartelt, E. T. Hoke, A. El Labban, P. M. Beaujuge, J. M. J. Frechet, M. D. McGehee, *Energy Environ. Sci.* **2013**, *6*, 2529.
[49] Y. Zhou, C. Fuentes-Hernandez, J. Shim, J. Meyer, A. J. Giordano, H. Li, P. Winget, T. Papadopoulos, H. Cheun, J. Kim, M. Fenoll, A. Dindar, W. Haske, E. Najafabadi, T. M. Khan, H. Sojoudi, S. Barlow, S. Graham, J.-L. Brédas, S. R. Marder, A. Kahn, B. Kippelen, *Science* **2012**, *336*, 327.
[50] F. Liu, Z. A. Page, V. V. Duzhko, T. P. Russell, T. Emrick, *Adv. Mater.* **2013**, *25*, 6868.
[51] S. Holliday, R. S. Ashraf, C. B. Nielsen, M. Kirkus, J. A. Röhr, C.-H. Tan, E. Collado-Fregoso, A.-C. Knall, J. R. Durrant, J. Nelson, I. McCulloch, *J. Am. Chem. Soc.* **2015**, *137*, 898.
[52] P. Cheng, H. Bai, N. K. Zawacka, T. R. Andersen, W. Liu, E. Bundgaard, M. Jørgensen, H. Chen, F. C. Krebs, X. Zhan, *Adv. Sci.* **2015**, *2*, 1500096.
[53] Y.-Y. Lai, Y.-J. Cheng, C. S. Hsu, *Energy Environ. Sci.* **2014**, *7*, 1866.
[54] L. Derue, O. Dautel, A. Tournebize, M. Drees, H. Pan, S. Berthumeyrie, B. Pavageau, E. Cloutet, S. Chambon, L. Hirsch, A. Rivaton, P. Hudhomme, A. Facchetti, G. Wantz, *Adv. Mater.* **2014**, *26*, 5831.
[55] W. Kim, J. K. Kim, E. Kim, T. K. Ahn, D. H. Wang, J. H. Park, *J. Phys. Chem. C* **2015**, *119*, 5954.
[56] D. H. Wang, A. Pron, M. Leclerc, A. J. Heeger, *Adv. Funct. Mater.* **2013**, *23*, 1297.
[57] A. Tournebize, A. Rivaton, H. Peisert, T. Chassé, *J. Phys. Chem. C* **2015**, *119*, 9142.
[58] A. J. Pearson, P. E. Hopkinson, E. Couderc, K. Domanski, M. Abdi-Jalebi, N. C. Greenham, *Org. Electron.* **2016**, *30*, 225.
[59] Y. Lin, J. Wang, Z.-G. Zhang, H. Bai, Y. Li, D. Zhu, X. Zhan, *Adv. Mater.* **2015**, *27*, 1170.
[60] Z. He, B. Xiao, F. Liu, H. Wu, Y. Yang, S. Xiao, C. Wang, T. P. Russell, Y. Cao, *Nat. Photonics* **2015**, *9*, 174.
[61] Y. Liang, Z. Xu, J. Xia, S.-T. Tsai, Y. Wu, G. Li, C. Ray, L. Yu, *Adv. Mater.* **2010**, *22*, E135.
[62] S.-H. Liao, H.-J. Jhuo, Y.-S. Cheng, S.-A. Chen, *Adv. Mater.* **2013**, *25*, 4766.
[63] T. S. van der Poll, J. A. Love, T. Q. Nguyen, G. C. Bazan, *Adv. Mater.* **2012**, *24*, 3646.
[64] B. Yu, X. Zhang, J. He, K. Yang, C. Zhao, *J. Appl. Polym. Sci.* **2008**, *108*, 3859.
[65] X. Lu, H. Hlaing, C.-Y. Nam, K. G. Yager, C. T. Black, B. M. Ocko, *Chem. Mater.* **2015**, *27*, 60.
[66] T. Xiao, H. H. Xu, G. Grancini, J. Q. Mai, A. Petrozza, U. S. Jeng, Y. Wang, X. Xin, Y. Lu, N. S. Choon, H. Xiao, B. S. Ong, X. H. Lu, N. Zhao, *Sci. Rep.* **2014**, *4*, 5211.
[67] H.-C. Liao, C.-S. Tsao, T.-H. Lin, C.-M. Chuang, C.-Y. Chen, U. S. Jeng, C.-H. Su, Y.-F. Chen, W.-F. Su, *J. Am. Chem. Soc.* **2011**, *133*, 13064.
[68] B. A. Collins, Z. Li, J. R. Tumbleston, E. Gann, C. R. McNeill, H. Ade, *Adv. Energy Mater.* **2013**, *3*, 65.
[69] G. G. Malliaras, J. R. Salem, P. J. Brock, C. Scott, *Phys. Rev. B* **1998**, *58*, 13411.
[70] L. J. Huo, S. Q. Zhang, X. Guo, F. Xu, Y. F. Li, J. H. Hou, *Angew. Chem. Int. Ed.* **2011**, *50*, 9697.

© 2016 WILEY-VCH Verlag GmbH & Co. KGaA, Weinheim